



*Supplement of*

## **Statistical modelling and climate variability of compound surge and precipitation events in a managed water system: a case study in the Netherlands**

**Víctor M. Santos et al.**

*Correspondence to:* Víctor M. Santos (victor.malagon.santos@nioz.nl)

The copyright of individual parts of the supplement might differ from the article licence.

## Introduction

This Supplementary Material is structured in three sections. Section 1 covers relevant aspects of copula theory to better understand how the 2D and 3D copulas are obtained in this study. Section 2 presents a theoretical example to illustrate the impact that conditioning the predictors on the impact variable has on the correlation coefficient and dependence patterns. Finally, Section 5 3 includes supplementary figures (S1-S13) that were referred to in the manuscript.

Sklar (1959) describes the connection between a Copula  $C$  and a bivariate cumulative distribution function (CDF)  $F_{XY}(x, y)$  of any pair of variables  $(x, y)$  as:

$$F_{XY}(x, y) = C[F_X(x), F_Y(Y)] \quad (1)$$

10 where  $F_X(x)$  and  $F_Y(y)$  are the univariate marginal distributions. The bivariate probability density function (PDF) has the following form:

$$f_{XY}(x, y) = C[F_X(x), F_Y(Y)]f_X(x)f_Y(y) \quad (2)$$

where  $f_X(x)$  and  $f_Y(y)$  represent the marginal PDFs.

In higher dimensions, a joint probability distribution is obtained via pair-copula constructions, i.e., Vine Copulas (Aas 15 et al., 2009; Schepsmeier et al., 2018). This construction is hierarchical in nature and provides higher flexibility than other multivariate distribution functions since different dependence structures between pairs of variables can be adopted. Assuming the joint CDF continuous with strictly increasing marginal CDFs, vine copulas allow for the decomposition of an  $n$ -dimensional copula density into the product of  $n(n-1)/2$  bivariate copulas. A decomposition example of a three-dimensional  $f(x_1, x_2, x_3)$  is given as:

$$20 \quad f(x_1, x_2, x_3) = f_{3|12}(x_3|x_2, x_1)f_{2|1}(x_2|x_1)f_1(x_1) \quad (3)$$

where:

$$f_{2|1}(x_2, x_1) = c_{12}(F_1(x_1), F_2(x_2))f_2(x_2) \quad (4)$$

$$f_{3|12}(x_3|x_2, x_1) = c_{13|2}(F_{1|2}(x_1|x_2), F_{3|2}(x_3|x_2))f_{3|2}(x_3|x_2) \quad (5)$$

$$f_{3|2}(x_3, x_2) = c_{23}(F_2(x_2), F_3(x_3))f_3(x_3) \quad (6)$$

$$25 \quad f(x_1, x_2, x_3) = f_3(x_3)f_2(x_2)f_1(x_1) \quad (7)$$

Therefore,  $f(x_1, x_2, x_3)$  can be expressed as:

$$f(x_1, x_2, x_3) = f_3(x_3)f_2(x_2)f_1(x_1) \text{ (marginals)} \quad (8)$$

$$\cdot c_{12}(F_1(x_1), F_2(x_2))f_2(x_2) * c_{23}(F_2(x_2), F_3(x_3))f_3(x_3) \text{ (unconditional pairs)} \quad (9)$$

$$\cdot c_{13|2}(F_{1|2}(x_1|x_2), F_{3|2}(x_3|x_2))f_{3|2}(x_3|x_2) \text{ (conditional pair)} \quad (10)$$

$$30 \quad f(x_1, x_2, x_3) = f_3(x_3)f_2(x_2)f_1(x_1) \quad (11)$$

## 2 Impact of predictors conditioning on correlation

Here we present a simple theoretical test to illustrate the impact that the predictors' conditioning (on the impact variable) has on the Kendall's rank correlation coefficient ( $\tau$ ) (Kendall, 1938). Let  $A$  and  $B$  be two variables with standard normal distribution

representing daily values of climate drivers. Let  $C$  be the impact variable driven by  $A$  and  $B$  by means of this simple impact<sup>3</sup> function  $C = A + B$ . The dependence pattern between  $A$  and  $B$  is modelled by a Gaussian copula with associated  $\tau$  ranging from -0.9 to 0.9. We define the predictand (impact variable) as the annual maximum of  $C$ , noted as  $C_{\max}$ , and the conditioned predictors as the values of  $A$  and  $B$ , respectively, when  $C_{\max}$  occurs, noted as  $A_{C_{\max}}$  and  $B_{C_{\max}}$ .

Figure S6 shows the scatter plots of randomly generated 50-year time series for each case and the corresponding conditioned predictors (in red). The corresponding empirically estimated  $\tau$  are also indicated. We can observe that when we condition on the impact variable (for which both drivers positively contribute) we extract a sub-sample of the drivers realizations for which the correlation experiences a negative shift (as compared to the original sample). It can be observed, for instance, that for independent drivers ( $\tau$  between  $A$  and  $B$  equals to zero, framed case in Figure S6) we obtain a negative  $\tau$  between the corresponding  $A_{C_{\max}}$  and  $B_{C_{\max}}$ . From the latter we could not conclude, therefore, that the drivers are negatively correlated (i.e. the probability of concurrent large values of both  $A$  and  $B$  being lower than what we would randomly get by chance). In that particular case, the drivers are actually independent. Only in the cases with very strong positive correlation between  $A$  and  $B$ , the associated  $\tau$  between  $A_{C_{\max}}$  and  $B_{C_{\max}}$  remains positive (in the example of Figure S6 for  $\tau \geq 0.6$  between  $A$  and  $B$ ). Therefore, a weak correlation between  $A_{C_{\max}}$  and  $B_{C_{\max}}$  does not necessarily imply a weak correlation between the underlying drivers. In fact, we argue that, for a given case, if the  $\tau$  between  $A_{C_{\max}}$  and  $B_{C_{\max}}$  is larger than the  $\tau$  between  $A_{C_{\max,\text{shuffled}}}$  and  $B_{C_{\max,\text{shuffled}}}$  as obtained from the corresponding independent case ( $A$  and  $B$  with the same marginal distributions but being the dependence pattern between them removed), then the underlying drivers  $A$  and  $B$  have a positive dependence pattern (i.e. concurrent large values of  $A$  and  $B$  are more likely to happen than by chance).

### 3 Figures

Included here are additional Supplementary Figures S1-S13 that were referred to in the manuscript.

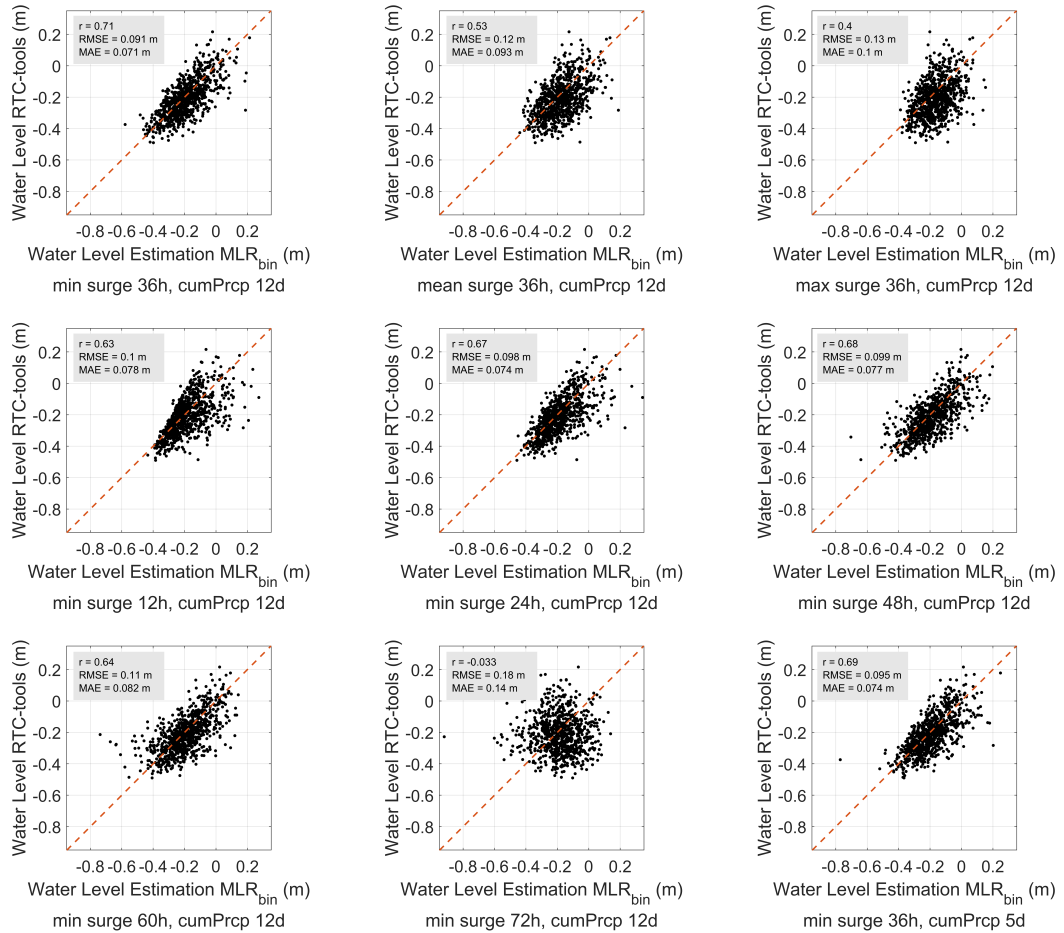


**Figure S1.**  $WL_{\max}$  obtained by RTC-tools vs.  $WL_{\max}$  obtained using the impact function based on Multiple Linear Regression with bin-sampling (MLR<sub>bin</sub>) and different sets of predictors.

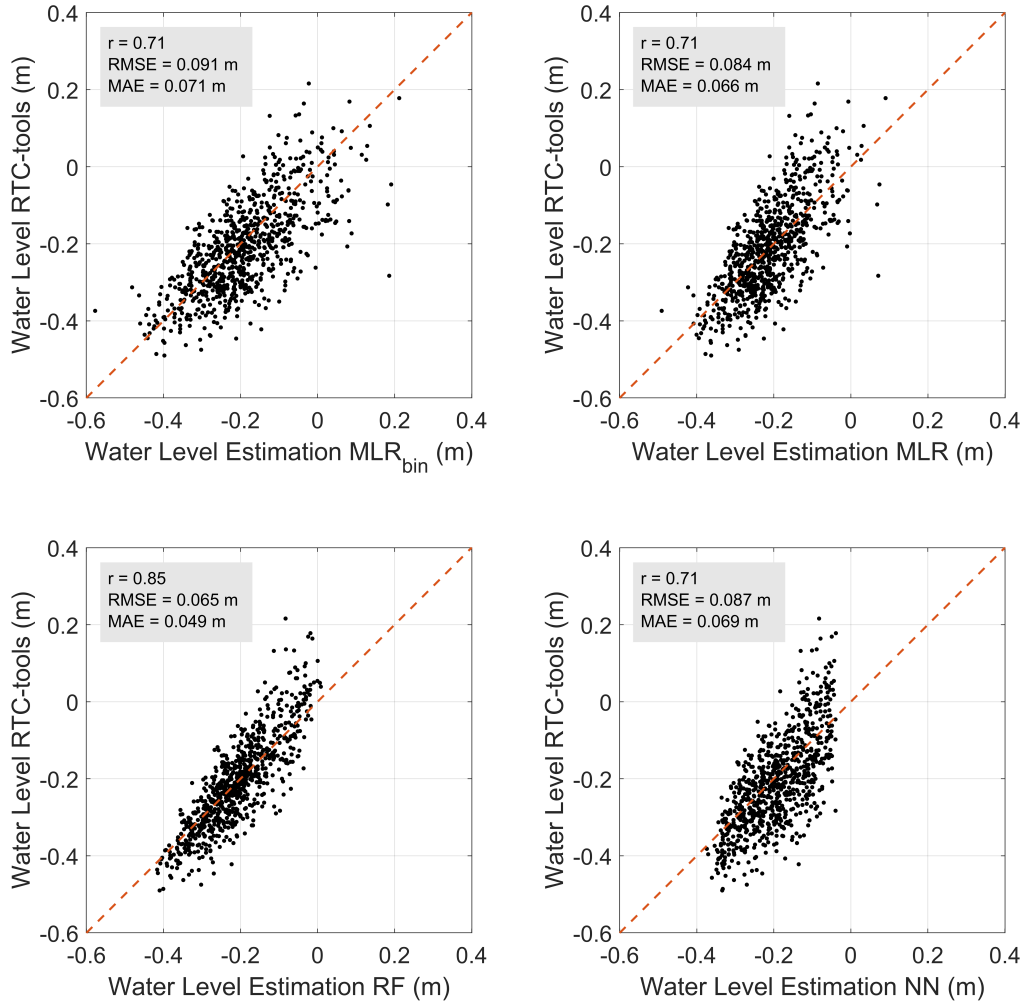


**Figure S2.**  $WL_{\max}$  obtained by RTC-Tools vs.  $WL_{\max}$  obtained using the following impact functions with  $S_{36h,\min}^T$  and  $P_{12d,\text{acum}}$  (2D case): Multiple Linear Regression with bin-sampling (MLR<sub>bin</sub>), Multiple Linear Regression (MLR), Random Forest (RF) and artificial Neural Networks (NN).

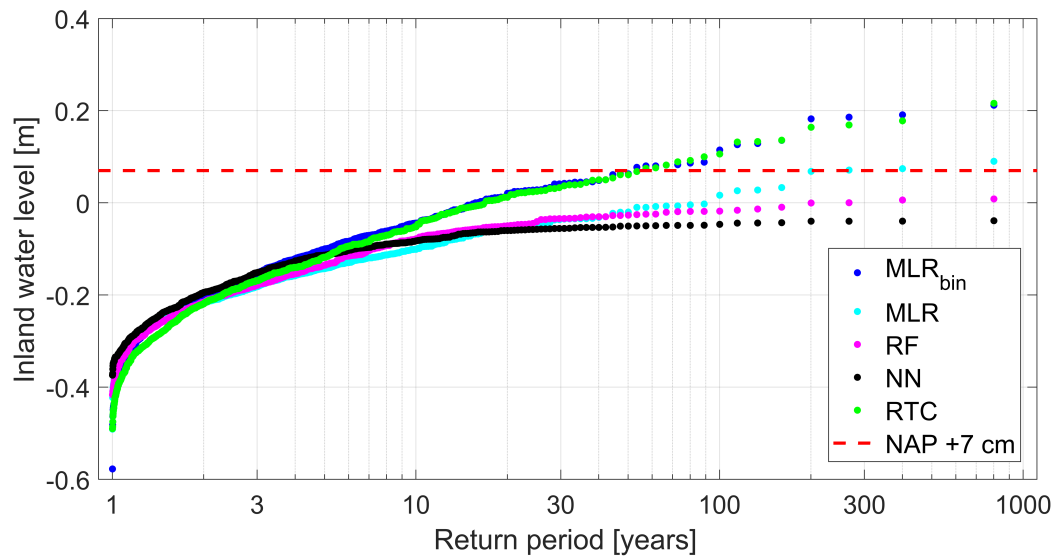


**Figure S3.** IWL return levels as generated from the RTC-Tools (green) and as obtained from the 2D case using the indicated impact functions: Multiple Linear Regression with bin-sampling (MLR<sub>bin</sub>), Multiple Linear Regression (MLR), Random Forest (RF) and artificial Neural Networks (NN). The red dashed line (NAP + 7 cm) represents the flood warning level.

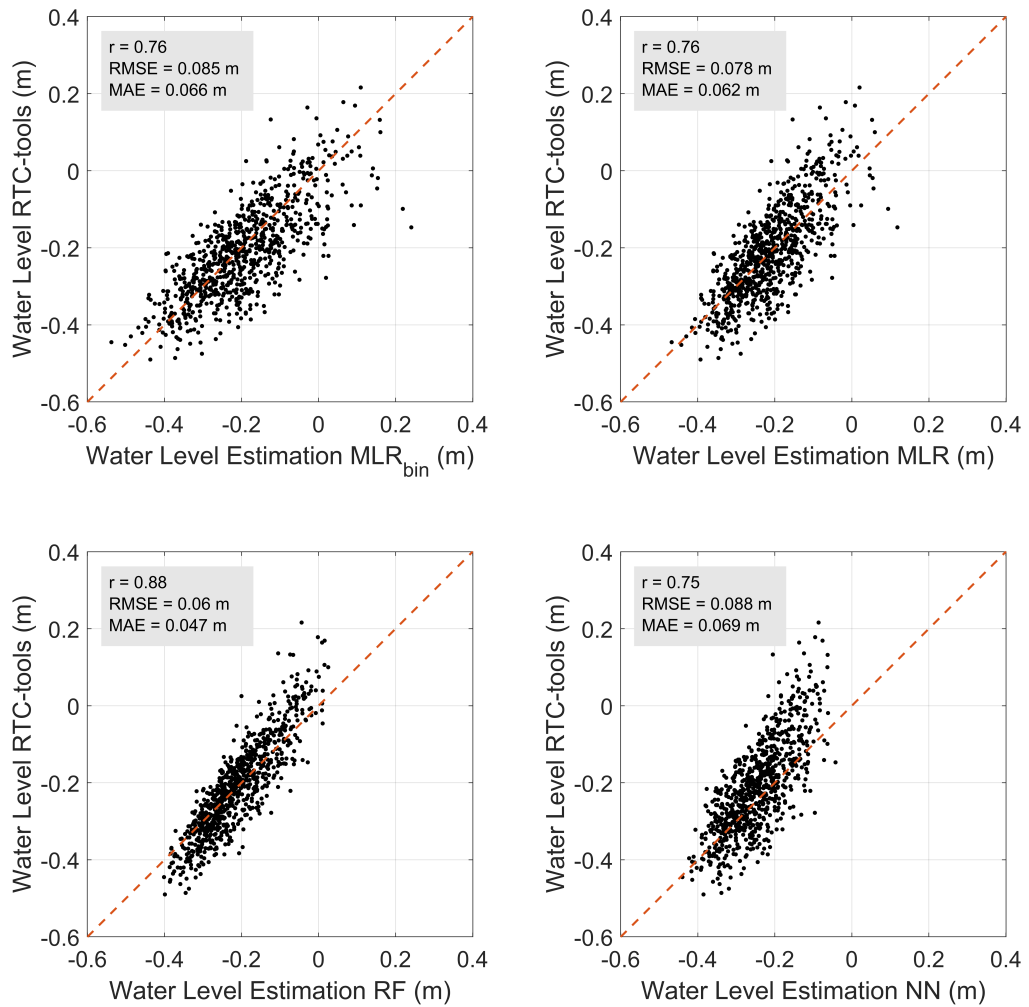


**Figure S4.**  $WL_{\max}$  obtained by RTC-Tools vs.  $WL_{\max}$  obtained using the following impact functions with  $S_{72h,\text{mean}}$ ,  $T_{12h,\text{min}}$  and  $P_{12d,\text{acum}}$  (3D case): Multiple Linear Regression with bin-sampling (MLR<sub>bin</sub>), Multiple Linear Regression (MLR), Random Forest (RF) and artificial Neural Networks (NN).

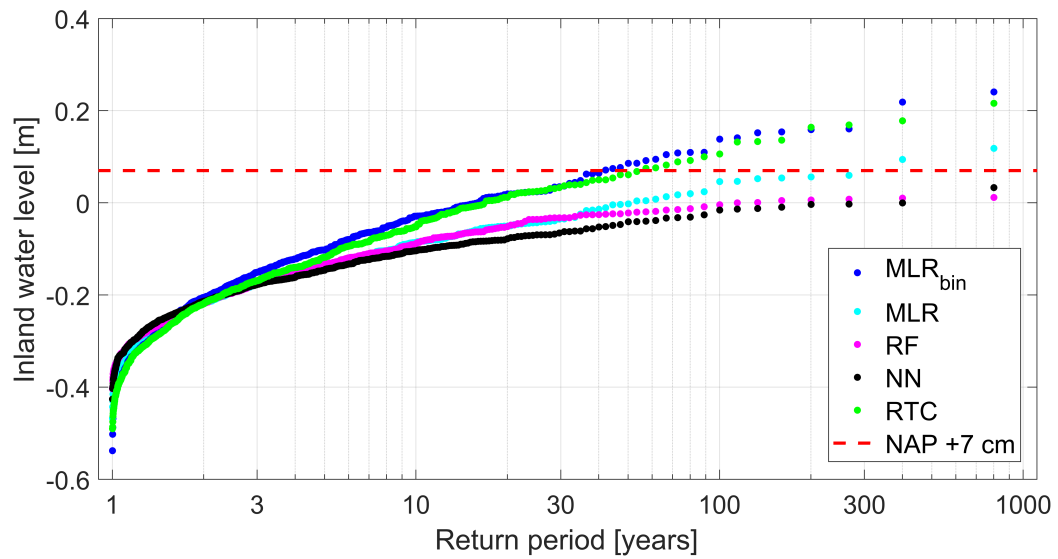


**Figure S5.** IWL return levels as generated from the RTC-Tools (green) and as obtained from the 3D case using the indicated impact functions: Multiple Linear Regression with bin-sampling ( $MLR_{bin}$ ), Multiple Linear Regression (MLR), Random Forest (RF) and artificial Neural Networks (NN). The red dashed line (NAP + 7 cm) represents the flood warning level.

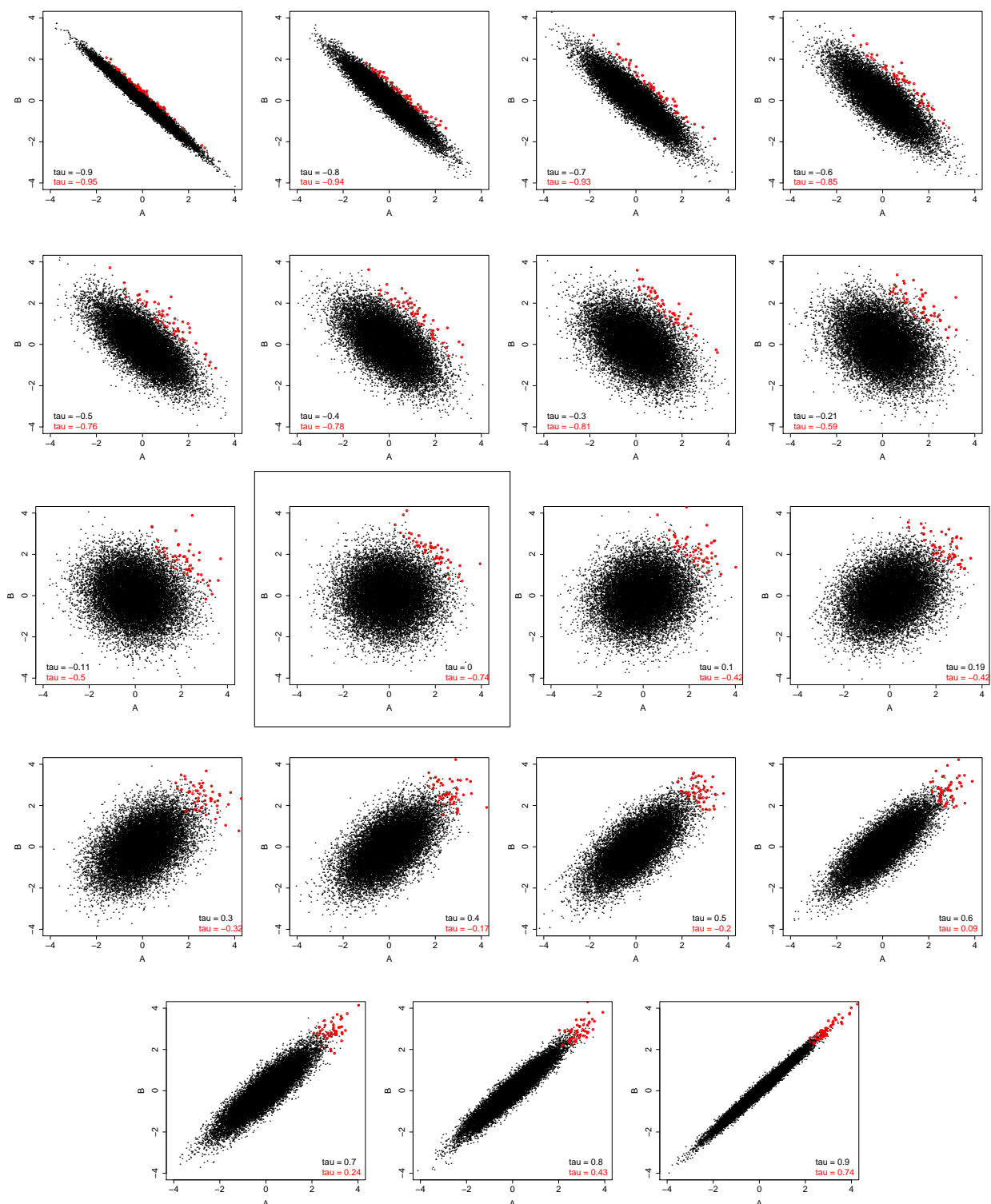


**Figure S6.** Scatter plot and estimated Kendall's  $\tau$  correlation coefficient for simulated drivers ( $A$  and  $B$ ) for different degrees of dependence (in black), and for conditioned predictors ( $A_{C_{\max}}$  and  $B_{C_{\max}}$ ) (in red). The independent case ( $\tau = 0$  between  $A$  and  $B$ ) is highlighted with a frame for reference.

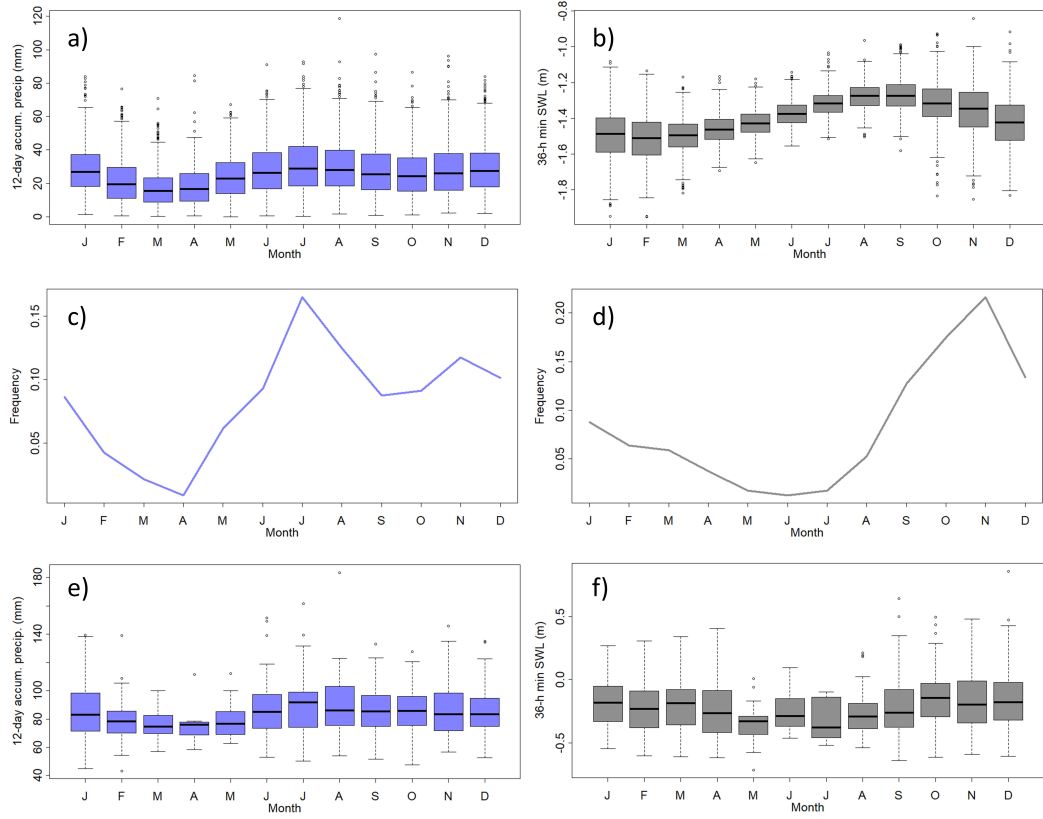


**Figure S7.** Seasonal statistics of the 12-day accumulative precipitation (blue color) and 36-h mean SWL (gray color): monthly maxima (a-b), monthly frequencies (c-d), and annual maxima. Note that here neither SWL nor precipitation is conditioned to the annual maximum IWL.

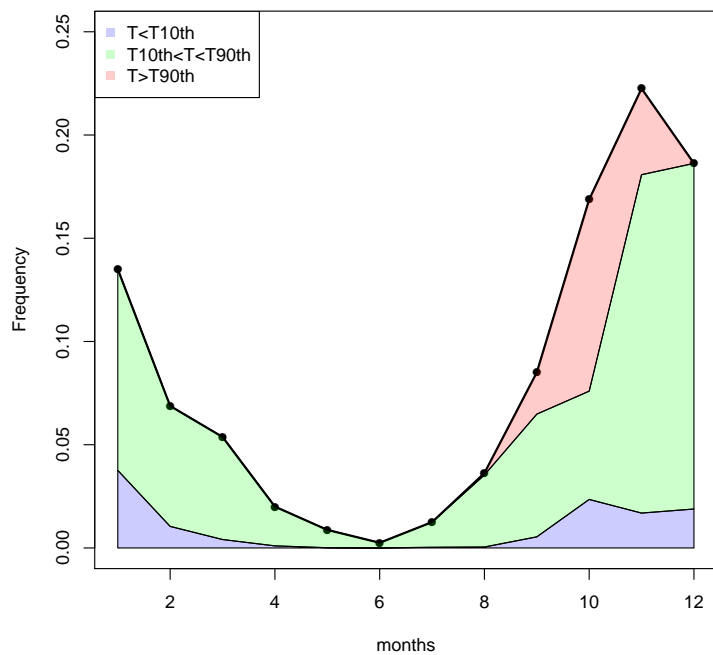


**Figure S8.** Monthly frequency of the tidal ranges indicated in the legend (shaded areas) relative to the total monthly frequency of  $WL_{max}$  events occurring each month (thick black line).

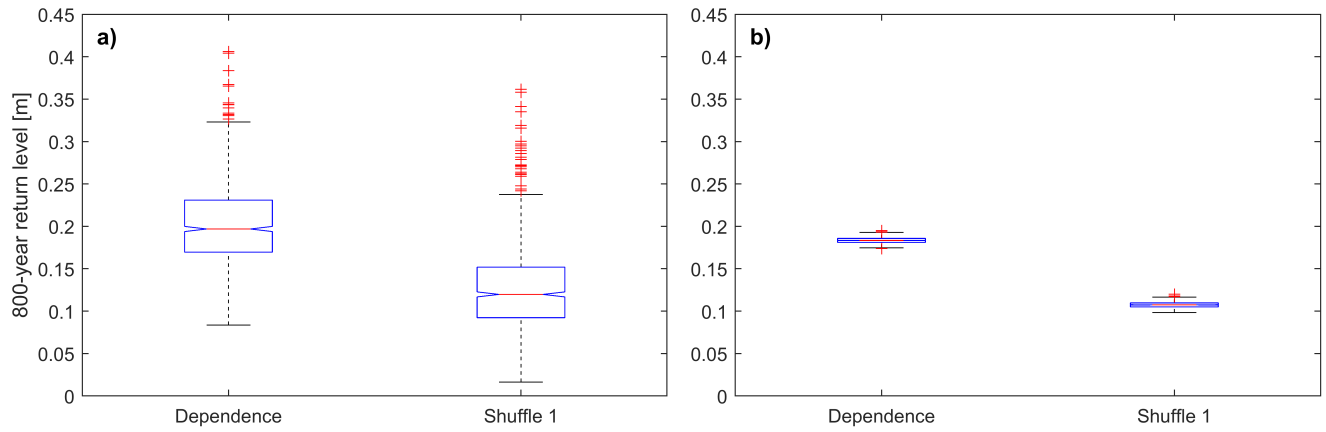


**Figure S9.** 800-year IWL return levels as obtained by calibrating the proposed statistical framework with original and shuffled data, respectively, and by simulating 800-yr(a) and 100,000-yr(b) records, respectively. Only the first 800-year permutation of the shuffled data is used here for illustration purposes.

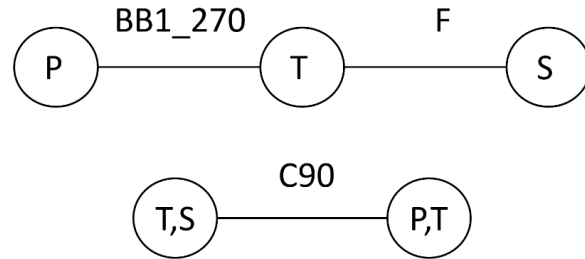


**Figure S10.** Structure of the regular vine obtained for the 3D dependence case.

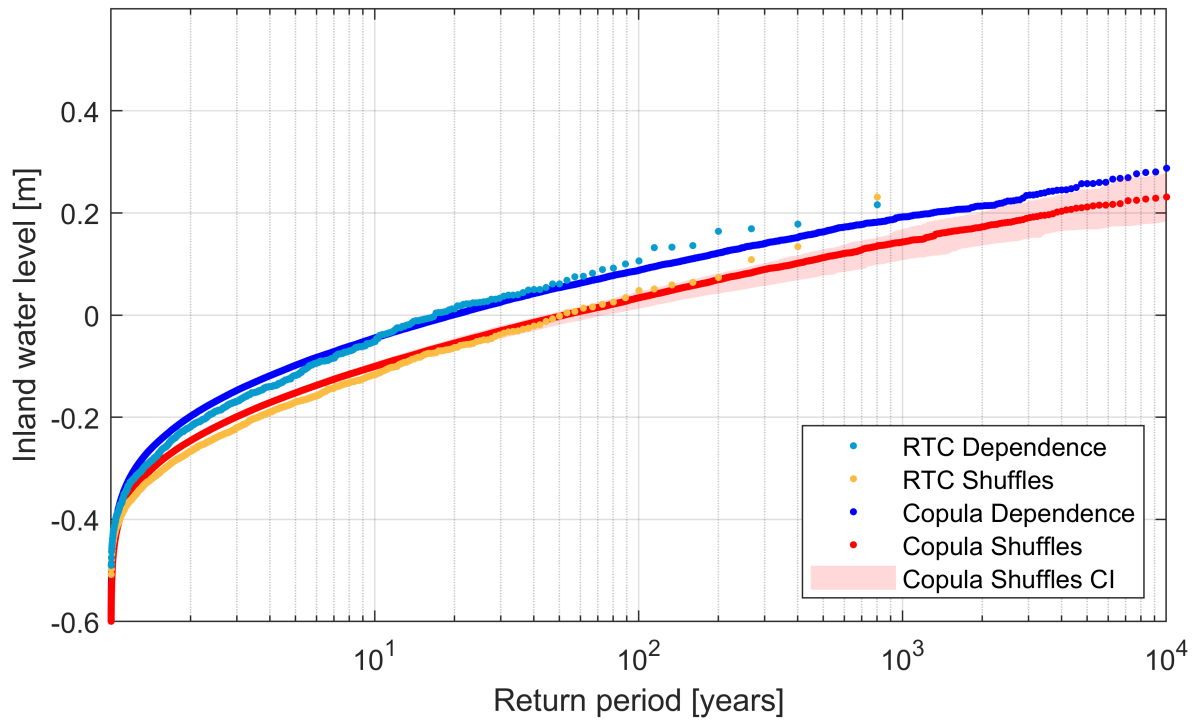


**Figure S11.** IWL return level against estimate return period using a trivariate copula model (3D case). Blue and red dotted lines depict the dependence and independence case, respectively. Transparent red denotes confidence intervals, which account for the uncertainty range between the 5<sup>th</sup> and 95<sup>th</sup> percentiles, as computed from all shuffles. Light blue and orange dots represent the curves empirically obtained.

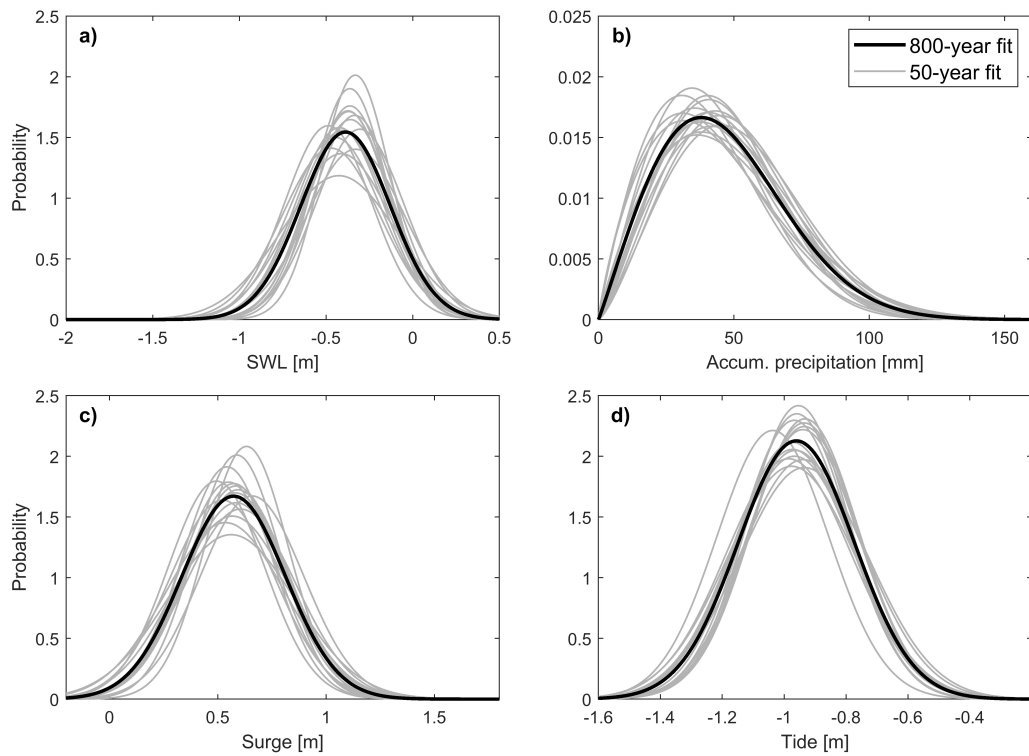


**Figure S12.** Variability of marginal probability density functions for 50-year runs (gray lines) and 800-year ensemble (black line) for the following predictors (original data): (a)  $S_{36h,\min}^T$ , (b)  $P_{12d,\text{acum}}$ , (c)  $S_{72h,\text{mean}}$ , (d)  $T_{12h,\min}$ .

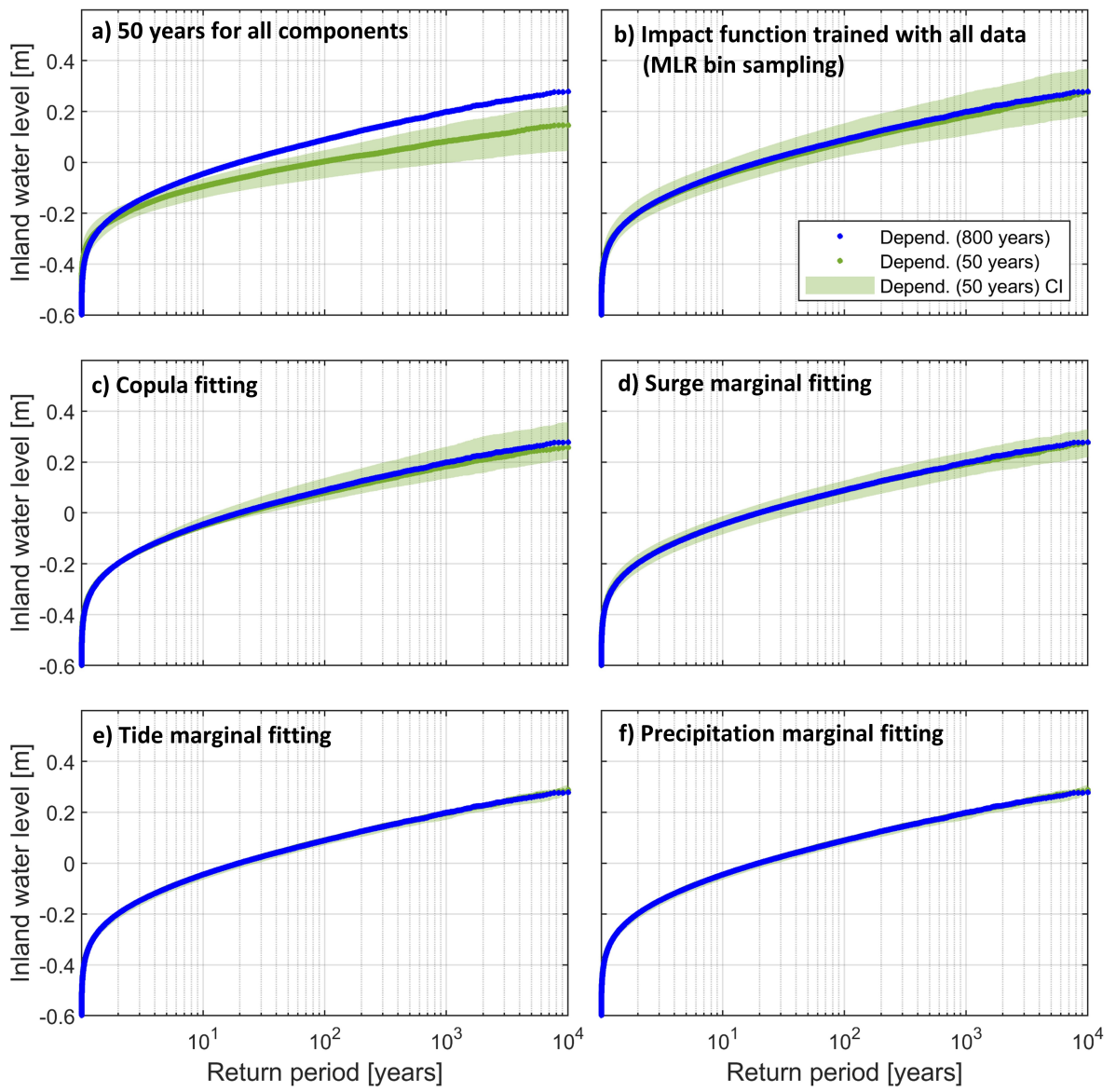


**Figure S13.** IWL return level against estimated return period using a trivariate (vine) copula. Blue dots depict the return level estimates obtained for the dependence using the proposed statistical framework. Transparent green illustrates the uncertainty associated to internal climate variability, represented by bounds computed using the 5th and 95th percentiles from all 50-year ensembles, and the median value (opaque green dots). Uncertainty is assessed for each component of the methodology: a) 50-year ensembles are used for all components; b) same as a) but impact function using the bin sampling approach is trained with 800 years of data; c) 50-year runs are used for copula fitting only; d) 50-year runs are used for surge marginal fitting only; e) 50-year runs are used for tide marginal fitting only; and f) 50-year runs are used for precipitation marginal fitting only.

55 Aas, K., Czado, C., Frigessi, A., and Bakken, H.: Pair-copula constructions of multiple dependence, *Insurance: Mathematics and economics*, 44, 182–198, 2009.

Kendall, M. G.: A new measure of rank correlation, *Biometrika*, 30, 81–93, 1938.

Schepsmeier, U., Stoeber, J., Brechmann, E., Graeler, B., Nagler, T., and Erhardt, T.: *Vinecopula: Statistical inference of vine copulas [Computer software manual]*, (R package version 2.1. 8), 2018.

60 Sklar, M.: Fonctions de repartition an dimensions et leurs marges, *Publ. inst. statist. univ. Paris*, 8, 229–231, 1959.